Geophys. J. Int. (2000) **143,** 937–944

Fault properties from seismic Q

M. H. Worthington[1] and J. A. Hudson[2]

[1] *T. H. Huxley School of Environment, Earth Sciences and Engineering, Imperial College of Science, Technology and Medicine, Prince Consort Road, London,* SW7 2BP, *UK. E-mail: m.worthington@ic.ac.uk*
[2] *DAMTP, University of Cambridge, Silver Street, Cambridge,* CB3 9EW, *UK. E-mail: j.a.hudson@damtp.cam.ac.uk*

Accepted 2000 September 13. Received 2000 September 13; in original form 1999 September 24

SUMMARY

A previously published investigation of seismic Q from a North Sea vertical seismic profiling data set has revealed an abrupt increase in attenuation to a Q-value of 45, which is associated with a region between 1000 and 2000 m depth where the borehole intersects a major fault zone dipping at approximately 50°. This Q anomaly is modelled using a linear slip theory. Fractures are considered to be imperfectly bonded interfaces where displacement is not required to be continuous. The resulting apparent attenuation of the vertically propagating incident P wave is shown to be very dependent on the dip angle of the fault, due to the relatively high predicted values of shear compliance compared to the normal compliance of fluid-filled fractures at 30–60 MPa confining pressure. The observed frequency independence of Q is satisfactorily reproduced. In addition to the low-pass filtering of the downgoing P wave, a difference in the frequency content of the first-arriving P wave on the vertical compared to the horizontal components has been observed. This difference is interpreted as resulting from Rayleigh scattering from 3-D inhomogeneities within the fault zone. No assumptions are required concerning the existence of intrinsic Q, although our results do not preclude this possibility.

Key words: attenuation, exploration seismology, fault models, Q, seismic wave propagation.

INTRODUCTION

Understanding the effects of faults and fractures on fluid flow behaviour and distribution within the crust is a matter of major current concern. In an introductory article for a special publication (Jones *et al.* 1998) devoted to this issue, Knipe *et al.* (1998) stated that compared to many other areas of petroleum geoscience, studies on the structural controls on fluid flow in hydrocarbon reservoirs are in their infancy. Plentiful evidence was then provided by other contributors in this volume regarding the extent of current knowledge and ignorance of the subject. Much useful data such as core and wireline logs were described that were obtained from boreholes that intersect faults. However, these borehole data alone are unlikely ever to provide unambiguous evidence about the potential for fluid flow along or across the fault within the broad vicinity of the hole or holes.

The aim of this paper is to investigate whether any useful information about the structure of faults and their average hydrological properties can be obtained from a study of the attenuation of seismic waves transmitted across a fault zone. We are specifically concerned with the analysis and interpretation of some vertical seismic profiling (VSP) data from a hole drilled through a major fault zone beneath the North Sea. Harris *et al.* (1997) have previously obtained estimates of seismic attenuation ($1/Q$) as a function of frequency and depth down this hole. Relatively high values of attenuation were obtained over the depth interval where the hole intersects the fault zone. This Q anomaly has clearly resulted from some change in the properties of the rocks. The key question is whether our current understanding of seismic wave propagation in inhomogeneous, anelastic media is sufficient for us to make some useful statement about what this change might be.

The main problem encountered when interpreting Q data is that results tend to be highly ambiguous due to the variety of totally different processes that can give rise to similar attenuation values. Seismic attenuation can conveniently be separated into two distinct classes, normally referred to as intrinsic attenuation and apparent attenuation. The former is a measure of the amount of energy that is irreversibly removed from a seismic wave as it propagates through an anelastic medium due to some energy conversion mechanism. The latter is an all-embracing term for any process that redistributes seismic energy in space and time but in which the total seismic energy is not diminished.

Intrinsic attenuation in vacuum-dry rocks is negligible (Q of hundreds or thousands) and increases markedly as soon as small amounts of fluid are introduced into the cracks and pores (Clark *et al.* 1981). The attenuation due to fluid flow through

interconnected pores, with or without viscous forces, was first studied by Biot (1956a,b). The effect of local squirting flow between thin cracks and equant pores has been investigated by Johnston *et al.* (1979), Murphy *et al.* (1986) and Mavko & Jizba (1991). Murphy *et al.* (1986) and Bourbie *et al.* (1987) provided reviews of the literature leading to the conclusion that fluid flow is the dominant intrinsic loss mechanism in sedimentary rocks. However, it has yet to be clearly established whether intrinsic attenuation is a significant or dominant mechanism at exploration seismic frequencies.

Gist (1994) introduced the concept of attenuation from pore-wall surface roughness and claimed to explain the experimental results of Klimentos & McCann (1990), who showed that the total clay content in sandstones plays an important role in ultrasonic attenuation. He also concluded that attenuation from all viscous dissipation mechanisms is negligible when scaled to the lower frequencies of field measurements. This conclusion is consistent with the results of a theoretical study by Peacock & Hudson (1990). They modelled viscous dissipation within fluid-filled cracks simply by adding an imaginary part, $i\omega\eta$, to the shear modulus of the crack-filling material, where η is the dynamic viscosity of the fluid. Pointer *et al.* (2000) described a theoretical investigation of three distinct mechanisms of fluid flow: flow through connections between cracks in an otherwise porous material, fluid movement within partially saturated cracks and diffusion from cracks into a porous matrix material. Results from this study indicate that these models can have a significant effect at frequencies of tens to hundreds of Hertz.

In this study we do not investigate the effects of intrinsic attenuation at all. For the purposes of the modelling, we assume that intrinsic Q is infinite. This does not preclude the possibility that intrinsic attenuation may be a partial cause of the observed low-Q zone. However, it is not a necessary condition.

Scattering is a word that is often associated with apparent attenuation, normally to imply a 2- or 3-D variation in elastic properties. The 1-D equivalent process, apparent attenuation due to interbed multiples, was first discussed by O'Doherty & Anstey (1971) and has subsequently been investigated by many others including Schoenberger & Levin (1978) and Shapiro & Hubral (1996). Another process that can result in apparent attenuation is the linear slip model (Schoenberg 1980; Schoenberg & Douma 1988; Pyrak-Nolte *et al.* 1990; Hudson *et al.* 1997; Verweij & Chapman 1997). Fractures or cracks are modelled as imperfectly bonded interfaces where displacement is not required to be continuous. Published applications of this model to real data are limited because in many cases, for reasons explained below, the effect is negligibly small, particularly at exploration seismic frequencies of 50–100 Hz. Pyrak-Nolte *et al.* (1990) have measured the compliance of fractured core samples. Myer *et al.* (1995) have performed a small-scale field experiment in fractured basalt. Seismic waves were transmitted between boreholes 3 m apart in a tunnel wall, both parallel and at right angles to a dominant fracture direction. The dominant frequency of the wavelet was approximately 40 kHz. Majer *et al.* (1997) have been able to image a near-surface fracture between two boreholes by recording transmission amplitudes before and after air was injected into the fault. They observed that the displacement of water by air in fractures, with a width of the order of a millimetre, produced large changes in the P-wave signal despite the wavelength of the signal being on the order of 0.5–1 m. One of the main objectives of this paper is to propose that the linear slip model could be more applicable to upper crustal conditions and low-frequency exploration seismic data than is commonly recognized.

There follows a description of the data analysed in this study. We then show how the observed low-Q anomaly could be due to linear slip at fracture planes within a fault zone. Evidence of Rayleigh scattering at 3-D structural inhomogeneities within the fault zone is also presented. We conclude with comments on some wider implications of this work with regard to the interpretation of crustal reflection seismic data.

THE DATA

The VSP data that we analyse were obtained from a vertical well in the North Sea. Fig. 1 shows the well location superimposed on a migrated reflection seismic time section. The region of interest in this study is the depth range from 1000 to 2000 m, which corresponds to two-way times in Fig. 1 from 800 to 1400 ms. This is the region where the well intersects a major fault zone, which is dipping at approximately 50° at the depth of intersection. The two horizontal arrows mark depths in the borehole where significant faulting has been identified. The rocks are predominantly sandstones, siltstones and claystones of Triassic and Lower Jurassic age. Also shown in the figure is the Q estimate obtained from the VSP data by Harris *et al.* (1997), hereafter referred to as the HKW Q model. The peak attenuation at approximately 1.2 s is a Q of 45. These authors describe a procedure for estimating the variation of Q with frequency but find little evidence of any frequency-dependent Q for these data over a bandwidth from 40 to 140 Hz. The Q profile in Fig. 1 is an average of their results over this bandwidth.

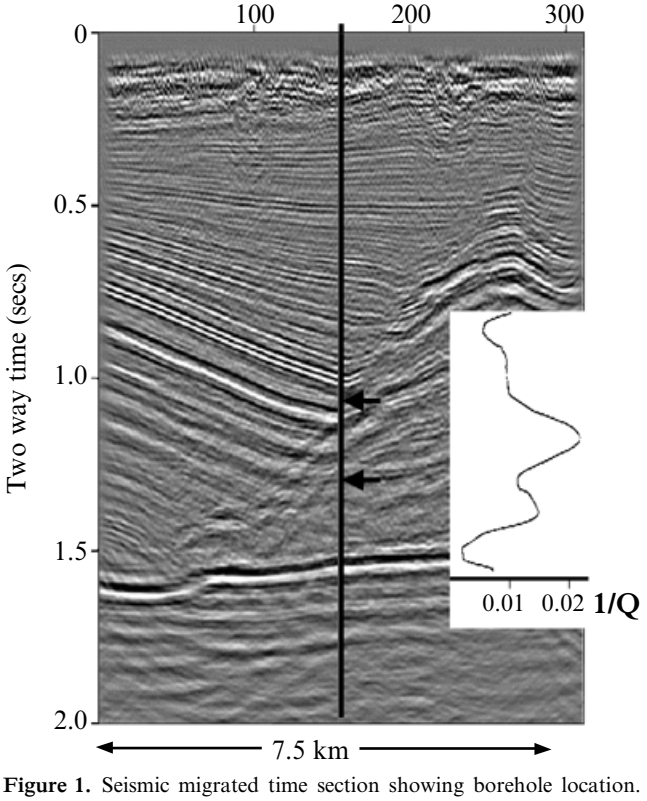

Figure 1. Seismic migrated time section showing borehole location. Arrows indicate positions of two major faults identified from the well logs. The $1/Q$ log from Harris *et al.* (1997) is superimposed.

Fig. 2 shows the portions of the VSP data that we analyse. Some pre-processing, as fully described in Harris *et al.* (1997), has been applied to these data. Fig. 2(a) shows the vertical component and Figs 2(b) and (c) the horizontal components. Note the decrease in bandwidth with depth of the first-arrival wavelet on the vertical component (Fig. 2a). This is more clearly seen in Fig. 3(a), which shows the three-component data at 1000 and 2000 m depth. The relative amplitudes of the three components are plotted correctly. Fig. 3(b) shows the normalized frequency spectra of the traces in Fig. 3(a). Note that the bandwidth of the vertical component at 2000 m is significantly less than the bandwidth of the vertical component at 1000 m. However, the bandwidth of the vertical component at 1000 m is very similar to the bandwidth of the horizontal components at 2000 m. This process may extend over a larger depth interval because the horizontal components at 1000 m again have a broader bandwidth than their corresponding vertical component. It is possibly more convincing simply to look at the wavelengths of the first-arrival wavelet on the vertical and horizontal components at 2000 m, which are clearly different.

MODELLING

Linear slip

Elastic wave behaviour across an imperfectly bonded interface between two elastic media has been described by Schoenberg (1980) in terms of a linear slip model. The displacement across the interface is not required to be continuous. The displacement discontinuity, or slip, is taken to be linearly related by a factor known as the fault compliance to the traction, which is continuous across the interface. The continuity equations at such an interface with a normal in the x_3-direction of Cartesian coordinates may be written as

$$t_1 = \left(\frac{\omega\mu}{\alpha}\right) B_t[u_1],$$

$$t_2 = \left(\frac{\omega\mu}{\alpha}\right) B_t[u_2],$$

$$t_3 = \left(\frac{\omega\mu}{\alpha}\right) B_n[u_3], \quad (1)$$

where $\mathbf{t}$ is the traction on the interface (assumed continuous), $[\mathbf{u}]$ is the displacement discontinuity, B_t and B_n are non-dimensional stiffnesses (stiffness = 1/compliance), μ and α are the rigidity and P-velocity of the rock and ω is the angular frequency.

Reflection and transmission coefficients of P and S waves at such an interface are frequency-dependent. In particular, the P-wave transmission response has the characteristics of a low-pass filter, so a P wave transmitted through the interface will be attenuated. This falls under the category of apparent attenuation, since the total energy is conserved in the transmitted P, transmitted S, reflected P and reflected S waves (although energy absorption—intrinsic attenuation—can be introduced by the use of complex values for the compliances).

We model the observed attenuation of the downgoing P wave between 1000 and 2000 m depth by assuming that a fault or faults intersect the transmission path and by basing our estimates of compliance on the work of Hudson *et al.* (1997), in which a model of a fault where two faces do not exactly conform is characterized by a distribution of contact regions; elsewhere the faces are stress-free. Wavelengths are long compared to the scale lengths of the fault structure (diameter and spacing of the areas of contact) and a relatively small proportion

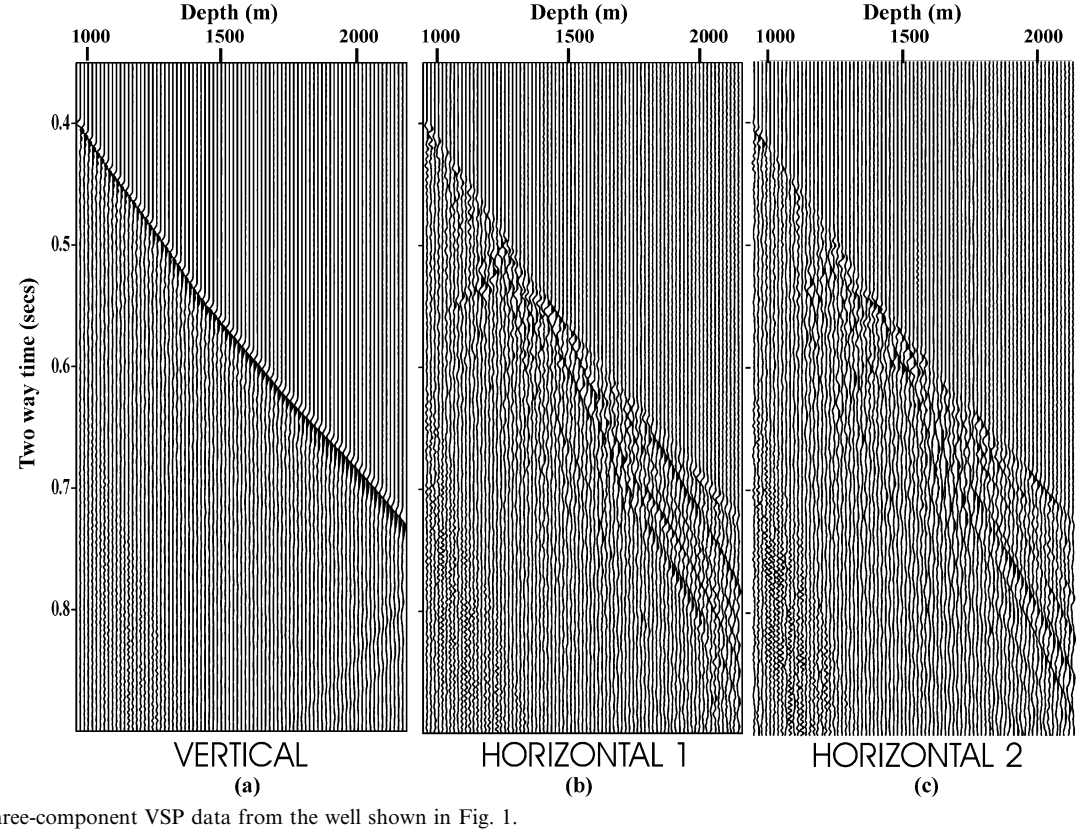

Figure 2. Three-component VSP data from the well shown in Fig. 1.

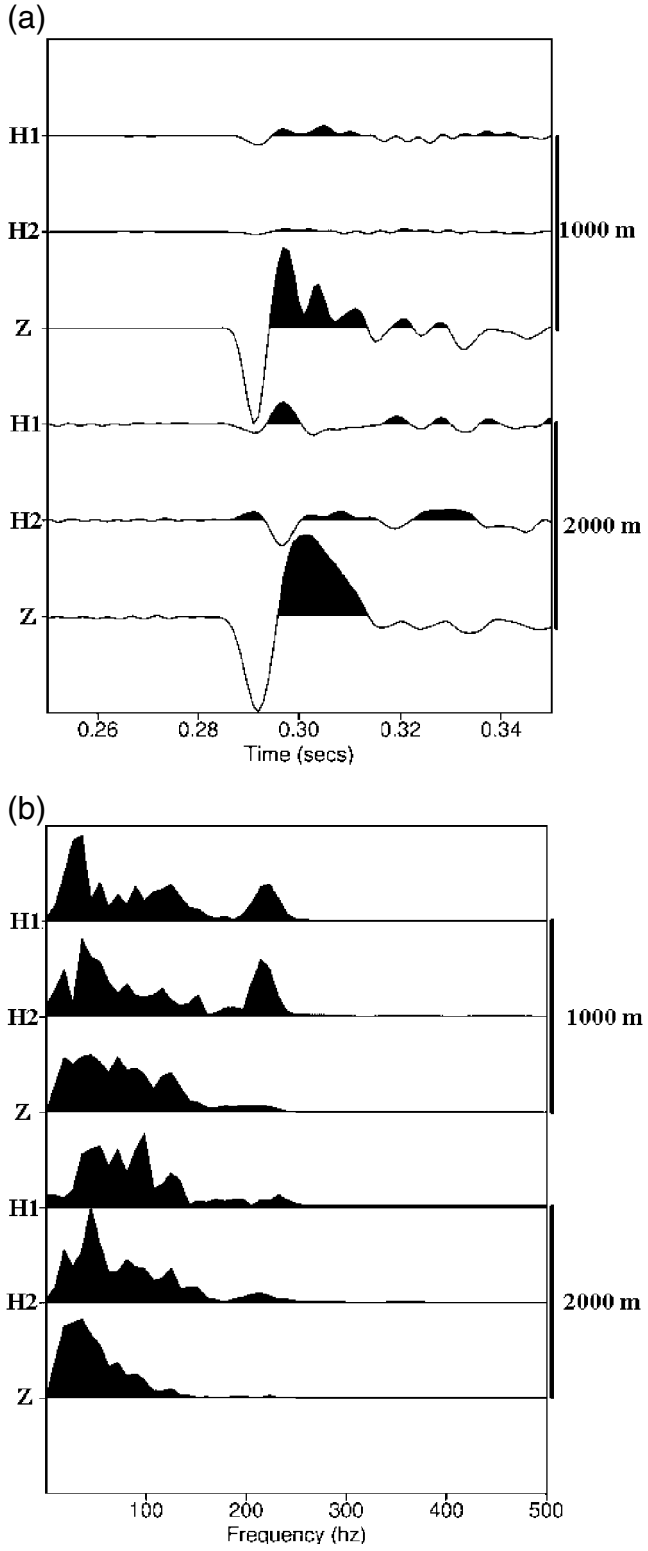

Figure 3. (a) Three-component VSP data at depths 1000 and 2000 m. (b) Amplitude spectra of the data in (a).

of the area of the fault surface is assumed to be in welded contact. This contrasts with the model in a related study by Hudson *et al.* (1996) in which the fault surfaces are pressed closer together and the slip areas are reduced to a distribution of open regions or cracks. A high proportion of the area of the fault surface is now assumed to be welded compared to the area of the cracks. Values for fault compliance that we have calculated using the Hudson *et al.* (1996) theory for a range of reasonable, and probably unreasonable, parameter values are of the order of 10^{-13} m Pa^{-1} or less, which results in a vanishingly small variation of transmission coefficient with frequency at exploration seismic frequencies. Note that to explain the Q observations discussed in this paper, we need values of compliance of the order of 10^{-9} m Pa^{-1} or greater. This is intuitively reasonable. One might expect a small effect when a wave crosses a boundary that it 'sees' as mostly solid rock. Both models described above are stochastic in the sense that the parameters relating to the fault structure in the resulting formulae are average values, for instance, the radius of the contact areas or of the cracks. The models are, in fact, formulated in terms of an *average contact* or *average crack*, both of which are taken to be circular.

There is scope for confusion, particularly for the geologically trained reader, from our use of the terms crack, fracture and fault. We refer to any imperfectly bonded interface that is large with respect to seismic wavelength as a fault. The fault zone that we are studying will undoubtedly consist of a large and probably rather complex network of faults or fractures. When we refer to cracks, we specifically mean open regions between areas of weld on the fault surfaces.

The equations for normal and tangential stiffness (1/compliance) derived in Hudson *et al.* (1997), with minor modifications to cover the case of wet cracks, are, respectively,

$$B_{\mathrm{n}} = r^{\mathrm{w}}\left(\frac{4}{\pi}\right)\left(\frac{\alpha}{\omega a}\right)(1-\beta^2/\alpha^2)\left\{1+\frac{2(r^{\mathrm{w}})^{1/2}}{\sqrt{\pi}}\right\}+\frac{\kappa'+(4/3)\mu'}{\Delta}, \tag{2}$$

$$B_{\mathrm{t}} = r^{\mathrm{w}}\left(\frac{8}{\pi}\right)\left(\frac{\alpha}{\omega a}\right)\frac{(1-\beta^2/\alpha^2)}{(3-2\beta^2/\alpha^2)}\left\{1+\frac{2(r^{\mathrm{w}})^{1/2}}{\sqrt{\pi}}\right\}+\frac{(\mu')}{\Delta}, \tag{3}$$

where α, β and μ are the P velocity, S velocity and rigidity of the rock, r^{w} is the proportion of the fault surface area that consists of welded contact, a is the mean radius of the contact areas, μ' and κ' are the rigidity and bulk modulus of the fault fill and Δ is the mean aperture of the fault. The derivation includes the assumption that r^{w} is less than about 0.2. We use these equations with the formulation in Schoenberg (1980) to calculate reflection and transmission coefficients.

Average estimates for P and S velocities of 4000 and 2350 m s^{-1} are obtained from the VSP data and an average density of 2.5 g cm^{-3}, and hence rigidity, is obtained from the borehole density log. We also estimate the dip of the fault zone from the seismic section and obtain a value of approximately 50° where it is intersected by the borehole. All other parameters must be estimated on the basis of the modelling.

A key observation resulting from eq. (2) is that normal compliance will always be much too small to be the cause of the Q anomaly that we observe. If the crack fill is a mixture of air and water, then, close to the Earth's surface, the introduction of a very small proportion of air (bulk modulus 1.0×10^5 Pa) will drastically reduce the bulk modulus of the air/water mixture since the bulk modulus of water is 2.25×10^9 Pa. Thus, gas-filled near-surface cracks can cause significant seismic attenuation, as has been shown by Majer *et al.* (1997). However, at a depth of approximately 1500 m, where the overburden pressure is approximately 40 MPa, the bulk modulus of any gas within a

temperature range of 0–300 °C will not be less than 10^8 Pa (Batzle & Wang 1992). So, even if our cracks are 100 per cent gas saturated, with κ' set to 10^8 Pa and a crack thickness of 1 mm, we obtain values for normal compliance of 10^{-13} m Pa^{-1} and the effect of the fault on the wave is vanishingly small.

However, when the angle of incidence with the fault is non-zero, the dominant parameter becomes tangential compliance rather than normal compliance. If we assume that the rigidity of the crack fill, μ', is zero, it follows from eq. (3) that the tangential compliance is independent of the thickness of the crack. Furthermore, for a fixed value of r^w, results are not critically dependent on the value of weld radius, a. Fig. 4(a) shows the variation of transmission coefficient with frequency and angle of incidence when $r^w = 0.1$, $a = 1.5$ m and $\mu' = 0$. Note that the transmission coefficient is effectively independent of frequency at normal incidence but that frequency dependence varies significantly with angle of incidence, due to the influence of the relatively high value of tangential compliance. Values of normal and tangential compliance for this model are 4.4×10^{-14} and 1.1×10^{-9} m Pa^{-1}, respectively.

Fig. 4(b) shows the variation of transmission coefficient with frequency and weld radius, a, when $r^w = 0.1$ and the angle of incidence is 50°. For a fixed value of r^w, the number of contact points per unit surface area tends to infinity as $a \to 0$, hence the stiffness of the fault increases and the transmission coefficient becomes frequency-independent. However, the frequency dependence of the transmission coefficient is relatively insensitive to changes in weld radius for values in excess of approximately 1.5 m.

The single key parameter controlling the magnitude of tangential compliance is thus the proportion of area of weld, r^w. Fig. 5(a) shows the amplitude spectra of the observed vertical-component P wavelets at 1000 and 2000 m. Also shown are the spectra resulting from filtering the data at 1000 m with the transmission response function shown in Fig. 4(a) for an incidence angle of 50°. This filtering is performed a number of times to simulate transmission across a set of approximately parallel similar faults. This is, of course, a fairly simple-minded way of calculating the effects of a sequence of slip planes. It is valid only if the multiples are well spaced so that the first arrival is not affected by interference. In other circumstances, the effect of multiple slip layers can be quite complex and would be sensitive to the specific geometry of the model. We bypass these details here in our search for a viable model that accounts for the data, but with the proviso that a more precise interpretation would need to investigate the effects of multiple interfaces in more detail.

The effects of two, five and 10 faults are shown in Fig. 5(a). Propagation through five faults is seen to be consistent with the observed seismic attenuation between 1000 and 2000 m depth. Fig. 5(b) shows the five-faults model and the real data plotted as log spectral ratios. The approximate linear slope between 20 and 120 Hz is consistent with Q being independent of frequency as was observed by Harris *et al.* (1997).

If r^w is increased to 0.2, the faults are stiffer, tangential compliance is reduced and propagation through 10 faults is required to achieve the same degree of attenuation. As already mentioned, eqs (2) and (3) are not strictly valid for values of r^w in excess of 0.2. In any event, our model becomes increasingly implausible for larger numbers of stiffer faults. It is not difficult to believe that the fault zone under investigation consists of a large number of faults. Steen *et al.* (1998) and Knipe *et al.* (1998) presented field examples of microfault densities within a zone 100 m either side of a fault of between 50 and 200 microfaults m^{-1}. However, such fault systems are normally highly complex, consisting of sets of fractures at differing angles to one another and to the average dip of the fault zone. In addition, these multiple fractures will not be large compared to the seismic wavelength or Fresnel zone radius and hence quite a different mathematical model would need to be used to study their influence. This could be a model giving rise to Rayleigh scattering.

In fact, we must explain why, in addition to the attenuation of the vertical component of the data, there is a difference in

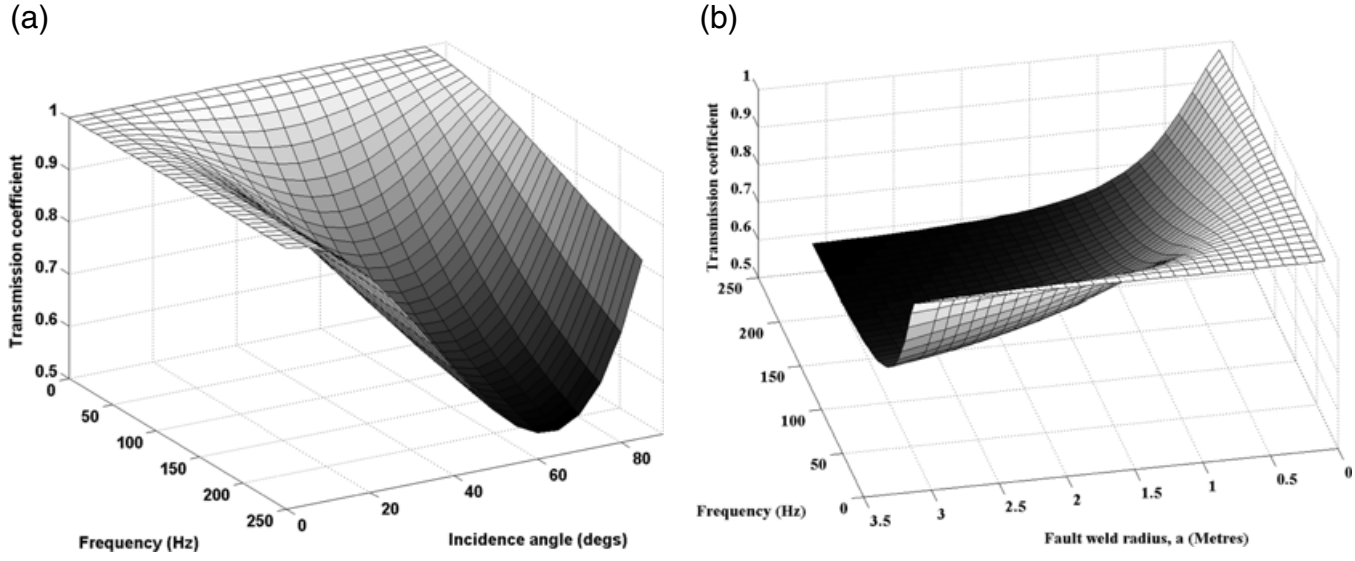

Figure 4. (a) *P*-wave transmission coefficient across a fluid-filled fracture as a function of frequency and angle of incidence of the *P* wave relative to the fracture plane. The area of weld is 10 per cent and the mean radius of welded contacts is 1.5 m. (b) *P*-wave transmission coefficient across a fluid-filled fracture as a function of frequency and mean radius, a, of welded contacts on the fracture surface. The area of weld is 10 per cent and the angle of incidence of the *P* wave relative to the fracture plane is 50°.

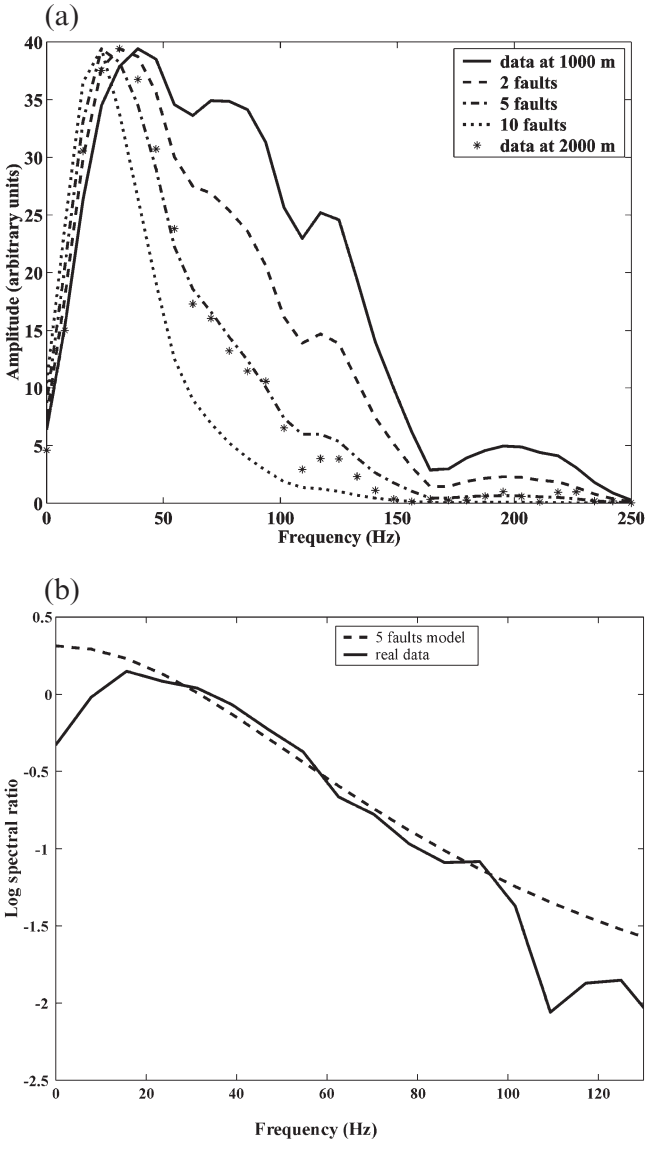

Figure 5. (a) Amplitude spectra of the *P* wavelet at 1000 m depth after propagation through two, five and 10 faults. (b) Log spectral ratio of the five-faults model and the real data at 2000 m in (a).

frequency content between the horizontal and vertical components of the data as illustrated in Fig. 3. Our proposed explanation is in terms of Rayleigh scattering from small-scale inhomogeneities.

3-D scattering

Any 3-D scattered energy from a predominantly vertically propagating wave will most easily be observed on a horizontal component geophone in a near-vertical borehole. We consider the simple model of a vertically propagating plane wave, incident on a layer of thickness h, in which bulk modulus, rigidity and density can vary with a correlation distance a and a normalized standard deviation σ; where

$$\sigma = \frac{\langle(\kappa-\kappa_0)^2\rangle^{1/2}}{\kappa_0}, \frac{\langle(\mu-\mu_0)^2\rangle^{1/2}}{\mu_0}, \frac{\langle(\rho-\rho_0)^2\rangle^{1/2}}{\rho_0}, \tag{4}$$

about mean values κ_0, μ_0 and ρ_0, where angular brackets imply spatial averaging. For in-phase reinforcement of the first half-cycle of the signal, the scattering has to come from an area of radius approximately w, where

$$w^2 = \frac{2\pi\alpha d}{\omega}, \tag{5}$$

α is the average *P*-wave velocity and d is the distance from the scattering layer to the receiver, assumed to be much larger than a wavelength. We postulate that the transverse signal that arrives at the same time as the *P* first arrival comes from side-scattered *P*. From Knopoff & Hudson (1964), we obtain the following root-mean-square amplitude of this transverse component for an incident plane wave of amplitude A_0:

$$A = A_0\pi^{5/4}\frac{\omega}{\alpha}\left(\frac{ha}{2}\right)^{1/2}\left(\frac{a}{d}\right)\sigma. \tag{6}$$

The wavelengths are assumed to be large compared to the correlation lengths of the scatterers. This is Rayleigh scattering with an ω^2 dependence for the amplitude. However, the area of scattering varies as $1/\omega$. Hence, the scattering amplitude is proportional to ω. Fig. 6 shows the spectrum of the wavelet on the vertical component at 1000 m, the spectrum after the operation of a *Q* filter of the form

$$\exp[-\omega d/2Q\alpha] \tag{7}$$

(*Q* is a simple average from the HKW *Q* model over the depth range 1000–2000 m and $d=1000$ m), and the spectrum after the operation of the *Q* filter plus the operator defined in eq. (6). Spectra have been normalized to enable the bandwidths of these data to be easily compared. Before normalization, the maximum amplitudes of these three spectra were in the ratio 1:0.63:0.08, respectively. Note the similarity between the spectral shape of the real data at 1000 m and these data after the application of the *Q* filter and the scattering operator in eq. (6). The increased scattering with frequency defined by eq. (6) is

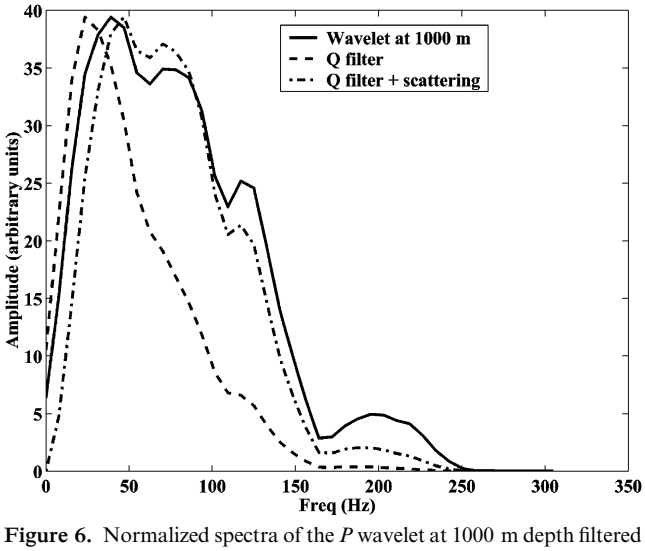

Figure 6. Normalized spectra of the *P* wavelet at 1000 m depth filtered with the scattering filter and the *Q* filter. See text for details.

compensating for the decrease of amplitude with frequency that is the result of eq. (7). This explains the similar bandwidths of the vertical component at 1000 m and the horizontal components at 2000 m in Fig. 3.

Values of A_0, a, h and σ in eq. (6) only affect the absolute amplitude, rather than the shape and bandwidth of the spectra. Consequently, the choice of these parameter values is not critical with regard to the conclusions of this experiment. However, to ensure that the absolute amplitude of our filtered data is approximately 1/10th of the amplitude of the input data, which is the same as the relative amplitudes of horizontal to vertical components at 2000 m, we choose $A_0 = 1$, correlation distance $a = 10$ m, scattering layer thickness $h = 800$ m and standard variation of elastic parameters $\sigma = 0.1$.

Note that we are proposing a composite model in which a small component of Rayleigh scattering is combined with a much more dominant attenuation mechanism that is due to linear slip at partially sealed faults.

DISCUSSION

We have shown that one explanation for the seismic attenuation between 1000 and 2000 m depth in our VSP data is that the vertical travelling P wave is low-pass filtered when passing through a zone of faulting due to displacement discontinuities at partially sealed fault surfaces. In addition a small amount of Rayleigh scattering accounts for the nature of the horizontal-component data. Any contribution due to intrinsic attenuation is assumed to be negligibly small.

It is important to appreciate that the physical model relating to the value of r^{w} (the proportion of the fault surface area that consists of welded contact) should not be taken too literally. Hudson & Liu (1999) have shown that exactly the same result could be derived if the irregular fault plane is replaced by a regular cubic packing of spheres. By so doing, they have demonstrated that the spatial distribution of the contact areas is not important. However, despite uncertainty about the precise geometry of the fault zone, it appears that there is a critical value of r^{w} of about 0.2 that represents the degree of openness of the fracture network. For values greater than this, seismic wave propagation through the cracks is effectively frequency-independent over a bandwidth from 0 to 300 Hz. Xu & King (1992) have also noted an exponential decrease in fracture compliance with increasing surface contact area.

Experimental or field data on the contact area of faults and how this varies with depth and fault size are very limited. Vandergraaf (1995) studied a natural fracture in a 1 m^3 granite block and reported a 10–15 per cent contact area. Keller *et al.* (1995) investigated a fracture in a 50×100 mm granite core and also observed a 10–15 per cent contact area. We have been unable to find any reports of fault contact areas at or near atmospheric pressure in excess of approximately 15 per cent. Pyrak-Nolte *et al.* (1987) determined variations of fracture contact area with normal stress for 52 mm diameter cores of granite. For two samples at 3 MPa effective stress, they obtained values of contact area of 8 and 15 per cent but these values increased to 30 and 42 per cent when the effective stress was 85 MPa. The normal stress–normal displacement behaviour of discontinuities can be highly non-linear. Brady & Brown (1985) described a hyperbolic relationship that included a maximum possible closure term that is independent of normal stress. Fracture properties in sedimentary, igneous and metamorphic rocks are known to be fractal (Yielding *et al.* 1992; Xie 1993), so it may be reasonable to extrapolate the results cited above to the scale of the fault zone in this study. Re *et al.* (1997) have studied variations in contact area as a function of joint size both experimentally and numerically by resorting to fractal geometry concepts. They found that the percentage of contact area decreased with increasing joint size. We conclude from these rather sparse data that a value of contact area in a large fault at 1.5 km depth of less that 20 per cent is possible but may be unusual.

Another consequence of the linear slip model is that seismic energy is conserved, so we might expect to observe transmitted and reflected S waves and reflected P waves that would have been generated at the fault surfaces. The depth interval of the fault zone is readily identified in the horizontal-component data in Figs 2(b) and (c) as a region of relatively high seismic complexity. Downgoing S waves can be seen originating from this region and some less coherent upgoing energy is also detectable, which may be P or S waves reflected close to the horizontal towards the borehole geophones. It would, of course, be surprising if reflected and refracted P and S waves were not generated within this rather complex fault zone simply because of acoustic impedance contrasts. Thus, all we are able to say is that the existence of these phases is at least not inconsistent with our model.

Other 3-D scattering mechanisms than the one considered above could be the cause of the HKW Q anomaly. Peacock & Hudson 1990) have calculated attenuation due to Rayleigh scattering and viscous dissipation in fluid-filled cracks but found that they were many orders of magnitude less than reported attenuations in the Earth. In addition to the question of magnitude, we are further constrained by the observations that the Harris *et al.* (1997) Q estimates are virtually independent of frequency over most of the bandwidth of the data and the primary downgoing wavelet remains quite simple over the entire depth range of interest. Groenenboom & Snieder (1995) proposed a multiple forward scattering approximation and were able to model significant attenuation of a P wavelet transmitted through distributions of scatterers. However, they did not claim to be able to model the whole signal, and the existence of high-amplitude coda waves in their synthetic seismograms is not consistent with our observations.

There is also the problem that most theories of scattering attenuation predict significant variations of Q with frequency. Most theories of intrinsic Q also require pronounced Q variation with frequency, normally with a steep decay either side of a resonance peak. Since frequency independence of intrinsic Q is a frequently observed phenomenon, it has been argued that the frequency independence results from the superposition of a range of relaxation peaks (Liu *et al.* 1976) or that the frequency dependence is within experimental error over the—normally—rather narrow frequency bands of field data (Sams *et al.* 1997). Precisely the same arguments can be applied to scattering Q. Instead of a relaxation peak at wavelengths approximately equal to the scatterer size, one can envisage scatterers with a range of sizes, so that $2\pi\alpha/\omega \approx a$ (the scatterer dimension or correlation length) for a range of values of ω.

However, we are not aware of any 3-D scattering theory that could explain all our observations: the observed low Q and frequency independence, the lack of pronounced coda after the downgoing vertical-component wavelet and the difference in frequency content between horizontal and vertical components.

ACKNOWLEDGMENTS

This work was carried out whilst MHW was on study leave, first at the Research School of Earth Sciences, Australian National University, Canberra, Australia, and then at Schlumberger Cambridge Research Ltd, Cambridge, UK. The hospitality offered by both Institutions is very much appreciated. The Australian study visit grant awarded by the Royal Society to MHW is gratefully acknowledged. The data were provided by Mobil North Sea Ltd and their support of this work is gratefully acknowledged.

REFERENCES

Batzle, M. & Wang, Z., 1992. Seismic properties of pore fluids, *Geophysics,* **57,** 1396–1408.

Biot, M.A., 1956a. Theory of propagation of elastic waves in a fluid saturated porous solid. I. Low frequency range, *J. acoust. Soc. Am.,* **28,** 168–178.

Biot, M.A., 1956b. Theory of propagation of elastic waves in a fluid saturated porous solid. II. Higher frequency range, *J. acoust. Soc. Am.,* **28,** 179–191.

Bourbie, T., Coussy, O. & Zinszner, B., 1987. *Acoustics of Porous Media,* Editions Technip, Paris.

Brady, B.H.G. & Brown, E.T., 1985. *Rock Mechanics for Underground Mining,* George Allen & Unwin, London.

Clark, V.A., Spencer, T.W. & Tittmann, B.R., 1981. The effect of thermal cycling on the seismic quality factor Q of some sedimentary rocks, *J. geophys. Res.,* **86,** 7087–7094.

Gist, G.A., 1994. Fluid effects on velocity and attenuation in sandstones, *J. acoust. Soc. Am.,* **96,** 1158–1173.

Groenenboom, J. & Snieder, R., 1995. Attenuation, dispersion and anisotropy by multiple scattering of transmitted waves through distributions of scatterers, *J. acoust. Soc. Am.,* **98,** 3482–3492.

Harris, P.E., Kerner, C. & White, R.E., 1997. Multichannel estimation of frequency-dependent Q from VSP data, *Geophys. Prospect.,* **45,** 87–109.

Hudson, J.A. & Liu, E., 1999. Effective elastic properties of heavily faulted structures, *Geophysics,* **64,** 479–485.

Hudson, J.A., Liu, E. & Crampin, S., 1996. Transmission properties of a plane fault, *Geophys. J. Int.,* **125,** 559–566.

Hudson, J.A., Liu, E. & Crampin, S., 1997. The mean transmission properties of a fault with imperfect facial contact, *Geophys. J. Int.,* **129,** 720–726.

Johnston, D.H., Toksoz, M.N. & Timur, A., 1979. Attenuation of seismic waves in dry and saturated rocks: II. Mechanisms, *Geophysics,* **44,** 691–711.

Jones, G., Fisher, Q.J. & Knipe, R.J., 1998. Faulting, fault sealing and fluid flow in hydrocarbon reservoirs, *Geol. Soc. Lond. Spec. Publ.,* **147,** 319.

Keller, A.A., Roberts, P.V. & Kitanidis, P.K., 1995. Prediction of single phase transport parameters in a variable aperture fracture, *Geophys. Res. Lett.,* **22,** 1425–1428.

Klimentos, T. & McCann, C., 1990. Relationships among compressional wave attenuation, porosity, clay content and permeability of sandstones, *Geophysics,* **55,** 998–1014.

Knipe, R.J., Jones, G. & Fisher, Q.J., 1998. Faulting, fault sealing and fluid flow in hydrocarbon reservoirs: an introduction, in *Faulting, Fault Sealing and Fluid Flow in Hydrocarbon Reservoirs,* eds Jones, G., Fisher, Q.J. & Knipe, R.J, *Geol. Soc. Lond. Spec. Publ.,* **147,** i–xxi.

Knopoff, L. & Hudson, J.A., 1964. Scattering of elastic waves by small inhomogeneities, *J. acoust. Soc. Am.,* **36,** 338–343.

Liu, H.P., Anderson, D.L. & Kanamori, H., 1976. Velocity dispersion due to anelasticity; implications for seismology and mantle composition, *Geophys. J. R. astr, Soc.,* **47,** 41–58.

Majer, E.L., Peterson, J.E., Daley, T., Kaelin, B., Myer, L.R., Queen, J., D'Onfro, P. & Rizer, W., 1997. Fracture detection using crosswell and single well surveys, *Geophysics,* **62,** 495–504.

Mavko, G. & Jizba, D., 1991. Estimating grain scale fluid effects on velocity dispersion in rocks, *Geophysics,* **56,** 1940–1949.

Murphy, W.F., Winkler, K.W. & Kleinberg, R.L., 1986. Acoustic relaxation in sedimentary rocks: dependence on grain contacts and fluid saturation, *Geophysics,* **51,** 757–766.

Myer, L.R., Hopkins, D., Peterson, J.E. & Cook, N.G.W., 1995. Seismic wave propagation across multiple fractures, in *Fractured and Jointed Rock Masses,* pp. 105–109, eds Myer, L.R., Cook, N.G.W., Goodman, R.E. & Tsang, C.F., Balkema, Rotterdam.

O'Doherty, R.F. & Anstey, N.A., 1971. Reflections on amplitudes, *Geophys. Prospect.,* **19,** 430–458.

Peacock, S. & Hudson, J.A., 1990. Seismic properties of rocks with distributions of small cracks, *Geophys. J. Int.,* **102,** 471–484.

Pointer, T., Liu, E. & Hudson, J.A., 2000. Seismic wave propagation in cracked porous media, *Geophys. J. Int.,* **142,** 199–231.

Pyrak-Nolte, L., Myer, L.R. & Cook, N.W.C., 1990. Transmission of seismic waves across single natural fractures, *J. geophys. Res.,* **95,** 8617–8638.

Pyrak-Nolte, L., Myer, L.R., Cook, N.G.W. & Witherspoon, P.A., 1987. Hydraulic and mechanical properties of natural fractures in low permeability rock, *Proc. 6th Int. Congress on Rock Mechanics, Montreal,* pp. 225–231.

Re, F., Scavia, C. & Zaninetti, A., 1997. Variation in contact areas of rock joint surfaces as a function of scale, *Int. J. Rock Mech. Min. Sci.,* **34**, paper no. 254, p. 526.

Sams, M.S., Neep, J.P., Worthington, M.H. & King, M.S., 1997. The measurement of velocity dispersion and frequency-dependent intrinsic attenuation in sedimentary rocks, *Geophysics,* **62,** 1456–1464.

Schoenberg, M., 1980. Elastic wave behavior across linear slip interfaces, *J. acoust. Soc. Am.,* **68,** 1516–1521.

Schoenberg, M. & Douma, J., 1988. Elastic wave propagation in media with parallel fractures and aligned cracks, *Geophys. Prospect.,* **36,** 571–590.

Schoenberger, M. & Levin, F.K., 1978. Apparent attenuation due to intrabed multiples, *Geophysics,* **43,** 730–737.

Shapiro, S.A. & Hubral, P., 1996. Elastic waves in finely layered sediments: the equivalent medium and generalised O'Doherty-Anstey formulas, *Geophysics,* **61,** 1282–1300.

Steen, O., Sverdrup, E. & Hanssen, T.H., 1998. Predicting the distribution of small faults in a hydrocarbon reservoir by combining outcrop, seismic and well data, in *Faulting, Fault Sealing and Fluid Flow in Hydrocarbon Reservoirs,* eds Jones, G., Fisher, Q.J. & Knipe, R.J, *Geol. Soc. Lond. Spec. Publ.,* **147,** 27–50.

Vandergraaf, T.T., 1995. Radionuclide migration experiments under laboratory conditions, *Geophys. Res. Lett.,* **22,** 1409–1412.

Verweij, M.D. & Chapman, C.H., 1997. Transmission and reflection of transient elastodynamic waves at a linear slip interface, *J. acoust. Soc. Am.,* **101,** 2473–2483.

Xie, H., 1993. *Fractals in Rock Mechanics,* Balkema, Rotterdam.

Xu, S. & King, M.S., 1992. Modelling the elastic and hydraulic properties of fractured rocks, *Mar. Petrol. Geol.,* **9,** 155–166.

Yielding, G., Walsh, J. & Watterson, J., 1992. The prediction of small-scale faulting in reservoirs, *First Break,* **10,** 449–460.